Phys Chem Minerals (1992) 19:220–228

PHYSICS AND CHEMISTRY OF MINERALS
© Springer-Verlag 1992

Oxidation Kinetics of Fayalite (Fe_2SiO_4)

Stephen J. Mackwell

Department of Geosciences, The Pennsylvania State University, University Park, PA 16802, USA

Received October 18, 1991 / Revised, accepted March 23, 1992

Abstract. Single crystals of fayalite (Fe_2SiO_4) have been oxidized either in the hematite or the magnetite stability field to investigate the kinetics and mechanisms of oxidation. For samples heated in air at 770° C, a two-phase region composed of fine-grained iron oxide and silica phases formed as the reaction front moved into the sample, and an iron oxide layer formed external to this two-phase region. The presence of the single-phase oxide layer coating the specimens indicates that oxidation occurs by the migration of iron from the fayalite to the gas-solid interface rather than by the movement of oxygen in the opposite direction. For oxidation in air, the kinetics followed a parabolic growth law, with the rate of oxidation limited by the diffusion of iron from the internal reaction front to the gas-solid interface through the iron oxide. When fayalite was oxidized in the magnetite stability field, using a CO/CO_2 gas mixture at 1030° C, oxidation was controlled by the reaction at the gas-solid interface, yielding an oxidation rate considerably slower than that predicted for diffusion-controlled growth of the oxide layer.

Introduction

Fayalite (Fe_2SiO_4) is an iron orthosilicate with the olivine crystal structure. The iron in fayalite can exist in either the 2+ or 3+ state, dependent on the nature of the crystallographic site and the oxygen activity. Ferrous iron (Fe^{2+}) resides almost exclusively in the octahedral cation sites. Electron paramagnetic resonance measurements indicate that ferric iron (Fe^{3+}) resides in both the octahedral cation sites and the tetrahedral cation (silicon) sites, with somewhat higher concentrations in the former (Nakamura and Schmalzried 1983; Gaite and Hafner 1984). The excess positive charge (electron hole) associated with the ferric iron in octahedral sites is quite mobile and can hop from ferrous iron to ferrous iron (Schock and Duba 1984; Sato 1986). Though not commonly, fayalite does occur in the earth, usually associated with magnetite Fe_3O_4, neither of which is stable in air.

The oxygen stability field of Fe_2SiO_4 is bounded under oxidizing conditions by the breakdown of fayalite into quartz plus magnetite at the quartz-fayalite-magnetite (QFM) phase boundary and under reducing conditions by the breakdown of fayalite into quartz plus iron at the quartz-fayalite-iron (QFI) phase boundary. These phase relationships at 1 atm pressure are plotted against oxygen fugacity and temperature (O'Neill 1987) in Fig. 1. Also plotted on this figure are the iron-wüstite (IW), wüstite-magnetite (WM) and magnetite-hematite (MH) phase boundaries (O'Neill 1988).

The oxidation of fayalite involves the reaction and decomposition of the fayalite within an oxidizing environment to form silica and iron oxide (magnetite and/or hematite). On the basis of research on the diffusion of silicon in Mg_2SiO_4 and $(Mg_{0.9}Fe_{0.1})_2SiO_4$ (Jaoul et al. 1981; Houlier et al. 1990), it is assumed that silicon ions in fayalite are essentially immobile under the experimental conditions of this study. Thus, the oxidation process is similar to that observed for the oxidation of wüstite to magnetite (Backhaus-Ricoult and Dieckmann 1986) or the oxidation of magnetite to hematite (Païdassi and Lopez 1958; Atkinson and Taylor 1985). In the oxidation of wüstite to magnetite, Backhaus-Ricoult and Dieckmann showed that oxidation occurs by the transport of iron ions through the magnetite and that the motion of anionic (oxygen) defects could be neglected. These researchers report that the transport of iron to the gas-solid interface occurred via the inward flux of cation vacancies at high oxygen activities and the outward flux of iron interstitials at low oxygen activities. In the oxidation of magnetite to hematite, Atkinson and Taylor (1985) showed that, although the reported values for tracer diffusion of oxygen and iron in hematite are quite similar, the oxidation proceeds by the transport of interstitial iron ions through the hematite from the internal reaction front to the gas-solid interface.

Although the oxidation of fayalite is more complex than the oxidation of iron oxides due to the presence

of silica, the silica acts as a static marker for the oxidation process. If the oxidation proceeds by the transport of oxygen into the fayalite, both silica and iron oxide will be found at the gas-solid interface. However, if the oxidation proceeds by transport of iron from the interior of the sample to the surface, a single-phase layer of iron oxide will cover a two-phase interior of silica plus iron oxide. Consequently, the immobile silica component provides a useful marker for the location of the original surface of the fayalite and permits a definitive test of the oxidation mechanism.

Oxidation experiments have previously been performed on samples of natural olivine $(Mg_{0.9}Fe_{0.1})_2SiO_4$ to characterize the oxidation process in this geologically important material (Wu and Kohlstadt 1988). These experiments were performed in air at 700° to 1100° C for times from 0.5 to 100 h and show that magnesium and iron are transported through lattice and dislocation pipe diffusion, respectively, to the surface to form an external oxide layer. A three-phase layer is formed between the external oxide and the unoxidized olivine composed of SiO_2 and Fe_3O_4 precipitates within iron-depleted olivine. The kinetics of the oxidation are parabolic and are controlled by the lattice diffusion of magnesium. The experiments on fayalite reported here are much simpler in that the starting material is pure end-member fayalite, rather than a fayalite-forsterite ($Fe_2SiO_4-Mg_2SiO_4$) solid solution, and no internal oxidation products are expected or observed.

Kinetics of Oxidation

The oxidation of a metal or metal oxide involves the formation of an oxidized layer on the surface of the solid by the reaction between metal ions in the material with oxygen from the environment. This interaction can occur either at the surface of the oxide layer, when metal ions diffuse from the unoxidized solid through the oxide layer(s), or at the interface between the oxide and the unoxidized solid, when oxygen ions diffuse through the oxide layer(s) from the surface to the internal interface. The kinetics of the oxidation may be controlled either by the diffusion of ions through the oxide(s) or by the reaction at the gas-oxide interface or at the interface between the oxide and the unoxidized interior.

1. Growth of a Single Oxide Layer

In the case of diffusion-controlled oxidation, the rate of growth of the single oxide layer is directly dependent on the flux of ions through the oxide, either from the internal interface to the surface (of metal ions) or from the surface to the internal interface (of oxygen ions). In either case the flux, j_i, of the mobile ions is given by

$$j_i = -\frac{D_i C_i}{RT}\frac{d\eta_i}{dx} \tag{1}$$

for one-dimensional diffusion parallel to x in an isotropic medium. Here, D_i is the partial chemical diffusion coefficient, C_i is the concentration, and η_i is the electrochemical potential of the mobile species i (either oxygen or metal ions), and RT is the product of the gas constant and the absolute temperature. Thus, the flux of ions through the oxide layer and, hence, the rate of layer growth depend both on the diffusivity of the species and on the driving force (gradient of oxygen electrochemical potential) for diffusion. The growth rate of the external oxide layer is determined from the product of the flux and the molar volume V_m of the oxide:

$$\frac{d\Delta x}{dt} = j_i V_m \xi \tag{2}$$

where Δx is the thickness of the oxide layer at time t, and ξ is a stoichiometric coefficient equal to the number of moles of oxide formed per mole of species i transported across the oxide layer. As the layer grows thicker, the oxygen electrochemical potential gradient decreases, causing the flux to decrease with time. Because the difference in electrochemical potential across the oxide layer remains the same as the layer thickness increases, it can readily be shown from (1) and (2) that the layer thickness for diffusion-controlled oxidation will follow a law of the form

$$\Delta x^2 = 2 k_p t \tag{3}$$

where k_p is the parabolic rate constant (see e.g., Kubaschewski and Hopkins 1953; Schmalzried 1983). Such a law may also be expected when more than one chemical species are mobile.

Where an interaction at an interface controls the rate at which the oxidation proceeds, the growth of the oxide layer will be slower than for the diffusion-controlled case. Here, the bulk of the gradient in the oxygen electrochemical potential occurs across the interface. Thus, unlike the case for diffusion-controlled oxidation, the electrochemical potential gradient will remain constant with time and the oxide layer thickness will vary linearly with time

$$\Delta x = k_l t \tag{4}$$

where k_l is the linear rate constant. With time and increasing layer thickness, a slow change may be expected from linear to parabolic kinetics. During this transition period, no simple rate law is applicable. A linear increase in layer thickness with increasing time has been observed by Dieckmann et al. (1981), Backhaus-Ricoult and Dieckmann (1986) and Dieckmann (1987) for the oxidation of wüstite to magnetite, where the reaction of the iron cations with the CO/CO_2 at the sample surface rate limited the oxidation process.

2. Growth of Multiple Oxide Layers

When multiple oxide layers form during the oxidation of a solid, the kinetics of growth of the various layers are more complex than for a single oxide layer. Although

the chemical potential difference across each layer can be determined and the diffusivities for the mobile species may be known, the layer thickness is not defined simply by (2), as it is for the case of a single oxide layer. In this situation, only a component of the flux of mobile ions through a layer goes into the growth of that layer; the remainder reacts at the phase boundary to produce mobile species in the next layer. For example, in the oxidation of iron in air (Païdassi 1958a), wüstite (FeO), magnetite (Fe_3O_4), and hematite (Fe_2O_3) layers form between the unoxidized iron and the air at elevated temperatures. The growth of the oxide layers occurs by the diffusion of iron ions from the inner Fe – FeO boundary through the wüstite, magnetite and hematite layers to the surface. A component of the flux of iron ions goes into the growth of the wüstite layer at the FeO – Fe_3O_4 boundary; the remainder passes into the magnetite and diffuses to the Fe_3O_4 – Fe_2O_3 boundary where some component goes into the formation of magnetite, with the remainder passing into the hematite; this final component, having passed through the hematite layer reacts at the surface with oxygen to form Fe_2O_3, resulting in growth of this layer. Thus, the rate of growth of an individual layer in the multiple layer case is slower than when it is growing as a single oxide layer under the same chemical potential gradient (Atkinson and Taylor 1985).

When the formation of the oxide layers is diffusion controlled, the relative thickness of the oxide layers will depend on the diffusion rates of the mobile ions through the individual layers and on the chemical potential gradient across the layers (Kubaschewski and Hopkins 1953, p 137). Yurek et al. (1974) give a theoretical formulation for the relative thickness of oxide layers during the formation of a double oxide coating, which has been applied by Garnaud and Rapp (1977) and Atkinson and Taylor (1985) to the oxidation of iron. According to these treatments, when diffusion through a layer is particularly slow, that layer will be very thin, and may thus, for kinetic reasons, be undetectable. The relative thicknesses of the various layers are also generally independent of time. Under these circumstances, the growth of the individual layers and, hence, the growth of the entire oxide coating may be expected to follow a parabolic growth law such as (3).

Alternatively, if the reaction at a phase boundary rate limits the oxidation process in a system with multiple oxide layers, the rate of oxide growth will be slower than for diffusion-controlled growth and much of the chemical potential difference between the gas-solid interface and the innermost phase boundary may be expected to occur at that growth-limiting interface. The growth law for the total oxide coating may be expected to follow a linear growth law such as (4).

3. *Oxidation of Fayalite in Air*

In the following treatment of the kinetics of oxidation in fayalite, it is assumed that both silicon and oxygen ions are immobile and that only iron and electronic defects have appreciable mobility at the temperatures under consideration. This assumption is supported by the experiments reported below and agrees with previous reasearch on the oxidation of iron and the oxides of iron (e.g., Atkinson and Taylor 1985).

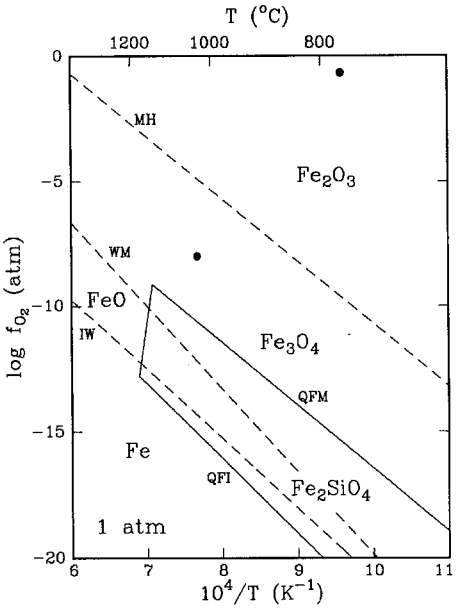

Fig. 1. Phase diagram in temperature and oxygen fugacity space for fayalite and the iron-oxygen system. The stability field for fayalite is indicated by the solid lines, where QFI is the quartz-fayalite-iron and QFM is the quartz-fayalite-magnetite phase boundary (O'Neill 1987). The stability fields for the various iron oxides and metallic iron are bounded by the dashed lines, where IW is the iron-wüstite, WM is the wüstite-magnetite, and MH is the magnetite-hematite phase boundary (O'Neill 1988). The filled circles indicate the oxygen fugacities and temperatures for the two sets of experiments

When fayalite is oxidized in air, thermodynamic constraints indicate that the oxidized layer adjoining the unoxidized fayalite is magnetite plus silica, and that the iron oxide phase in contact with air is hematite (Fig. 1). Given these constraints, there are several possible morphologies for the structure and composition of the oxidized layers on the fayalite, depending on the relative growth rates of the layers containing hematite and magnetite. If the diffusion of iron through Fe_2O_3 is faster than through Fe_3O_4, we would expect to find an external single-phase Fe_2O_3 layer, a two-phase $Fe_2O_3 + SiO_2$ layer, and a two-phase $Fe_3O_4 + SiO_2$ layer against the fayalite. By contrast, if the diffusion of iron through Fe_2O_3 is slower than through Fe_3O_4, we would expect to find an external single-phase Fe_2O_3 layer, a single-phase Fe_3O_4 layer, and a two-phase $Fe_3O_4 + SiO_2$ layer against the fayalite. It is also possible, given the appropriate rates of iron transport through the various layers, that one of the layers may be vanishingly small, so that we would observe only two layers.

In all cases, the oxidation of fayalite in air begins at the air-fayalite interface, where the oxygen activity is high, and proceeds into the interior, where the oxygen activity is low. At the surface, oxygen molecules in the air react with iron cations to form a layer of hematite.

Atkinson and Taylor (1985) and Hoshino and Peterson (1985a, b) have shown that the mobile iron defects in hematite are ferric iron interstitials. These iron interstitials are produced in the sample interior due to the breakdown of magnetite to hematite at an oxygen activity corresponding to the magnetite-hematite phase boundary. Dieckmann and Schmalzried (1977) have shown that, at high oxygen activities within the magnetite stability field, the mobile iron defects in magnetite are iron vacancies. Although they measured a change from vacancy to interstitial diffusion for iron in magnetite at lower oxygen activities, extrapolation of the oxygen activity at which the change in mechanism occurs to 770° C indicates that interstitial diffusion of iron only becomes important at oxygen fugacities near the quartz-fayalite-magnetite phase boundary (and does not become important at all for the experiments performed in CO/CO_2 at 1030° C). The iron vacancies in the magnetite are consumed at the internal interface where fayalite decomposes to form magnetite and silica at an oxygen activity corresponding to the quartz-fayalite-magnetite phase boundary.

Given the densities of the respective phases and the possible morphologies for the oxidation products, the thickness of the external oxide layer(s) should be approximately 18–25% of the thickness of the two-phase iron oxide plus silica layer(s), assuming that the layers are all fully dense. Also, the volume of the two-phase layer(s) should be approximately 92–97% of the thickness of the fayalite that is consumed during oxidation.

4. *Oxidation of Fayalite in CO/CO_2*

For the oxidation of fayalite in the magnetite stability region, oxygen molecules in the gas react with iron cations at the surface to form a layer of magnetite. At high oxygen activities, the mobile iron defects in magnetite are iron vacancies (Dieckmann and Schmalzried 1977; Dieckmann 1982). These iron vacancies are consumed at the internal interface where fayalite decomposes to form magnetite plus silica at an oxygen activity corresponding to that for the quartz-fayalite-magnetite phase boundary. During the oxidation of the fayalite in the magnetite stability field, three discrete zones should be visible in a cross section of the sample: an external magnetite layer, a layer of magnetite plus silica, and the unreacted fayalite, according to

$$2O_2 + 6Fe_2SiO_4 \rightarrow (3Fe_3O_4 + 6SiO_2)_{\text{two-phase}} + (Fe_3O_4)_{\text{external}}$$

Thus, for every 6 moles of fayalite that is oxidized, 1 mole of magnetite is added to the external oxide layer. Given the densities of the respective phases, the thickness of the external magnetite layer should be approximately 17% of that for the two-phase magnetite plus silica layer, assuming that both regions are fully dense. Also, the two-phase layer should be approximately 97% of the thickness of the fayalite that is consumed during oxidation.

Experimental Techniques

1. *Starting Material*

Fayalite samples were prepared from a synthetic single crystal, grown by the Czochralski method (Finch et al. 1980; Ricoult and Kohlstedt 1985) at an oxygen fugacity of 10^{-10} atm to ensure that most of the iron was in the divalent state. Other than a few small iron oxide (probably magnetite) precipitates, which were avoided in the preparation of the samples, the crystal was single-phase (Finch et al. 1980). Only a small number of oxidation experiments could be performed as there was very little of the synthetic fayalite. Natural fayalite contains a considerable proportion of additional phases, mostly magnetite, which makes it unsuitable for this type of study. The samples were cut to approximately $1 \times 1 \times 0.5\ mm^3$ prisms using a fine diamond-imbedded wire saw. The $1 \times 1\ mm^2$ surfaces were then polished to 0.05 μm with alumina powder.

2. *Experimental Conditions*

The oxidation experiments were performed in a 1 atm furnace with a vertical alumina tube and gas seals at either end to allow control of the gas mixtures around the samples. The oxygen fugacity around the samples was continuously monitored with an in situ zirconia oxygen fugacity sensor. Each sample was placed on a bed of coarse fragments of ferromagnesium olivine within a small alumina crucible that was attached to a thermocouple and suspended, through an o-ring seal, from the top of the furnace tube. The chromel/alumel thermocouple junction was located adjacent to the sample. During the experiment, the crucible was lowered rapidly into the furnace for the allocated time and then rapidly withdrawn. In this way, the uncertainty in the time-at-temperature could be constrained to less than 60 s. At the relatively low temperatures of these experiments, no chemical interaction between the ferromagnesium olivine and the sample was expected or observed.

Experiments were performed on single crystal samples of synthetic fayalite under two sets of conditions:

i) The first suite of oxidation experiments was performed at 770 ± 5° C, with the samples oxidized in air so that the oxygen fugacity was fixed at 0.21 atm. Under these conditions, hematite is the stable iron oxide phase and the oxygen fugacity around the sample is about 15 orders of magnitude more oxidizing than the QFM buffer at this temperature (4×10^{-16} atm) (Fig. 1). Experiments were performed for times from 1 to 100 hours.

ii) The second suite of oxidation experiments was performed at 1030 ± 5° C, with the oxygen fugacity controlled with CO/CO_2 mixtures at 10^{-8} atm. This oxygen fugacity is near the middle of the magnetite stability region, and is about 500 times the oxygen fugacity necessary to oxidize fayalite at these conditions (2×10^{-11} atm) (Fig. 1). This series of experiments were performed for times from 0.1 to 69.2 hours.

After the experiments, the surfaces of the samples were investigated using a JEOL JSEM scanning electron microscope or a JEOL 733 Superprobe electron microprobe to determine the morphology and composition of the surface phases. Subsequently, the samples were carefully sandwiched between two olivine slices, to protect the sample surfaces during grinding and polishing, and mounted in epoxy. Each sample was then cut in half using a fine diamond saw, and the exposed cross section of the oxidized fayalite was polished to 0.05 μm with alumina powder. Care was necessary in both the mounting and polishing to prevent chipping or abrasion of the external oxide layer. The composition and thickness of the reacted layers in the exposed cross section of the sample were measured with the electron microprobe.

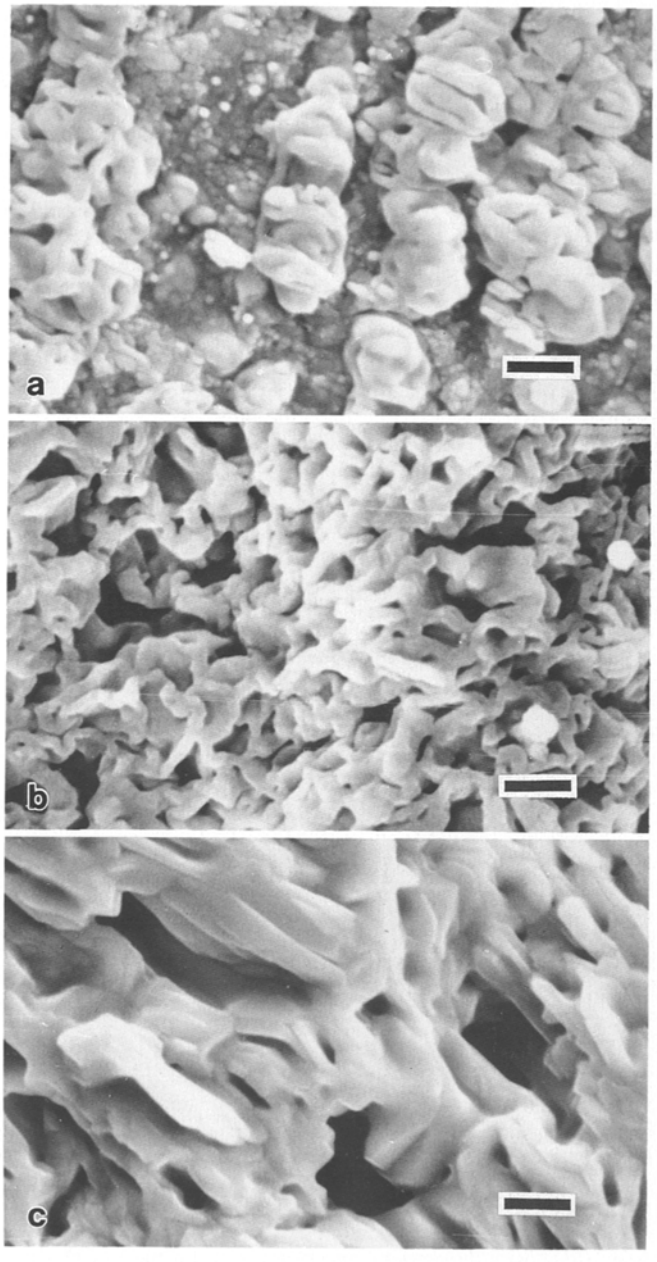

Fig. 2. SEI micrographs of the surfaces of samples that have been oxidized in air at 770° C, for **a** 1 h, **b** 10 h, **c** 100 h. 1 μm scale bars are shown in the lower right of each micrograph

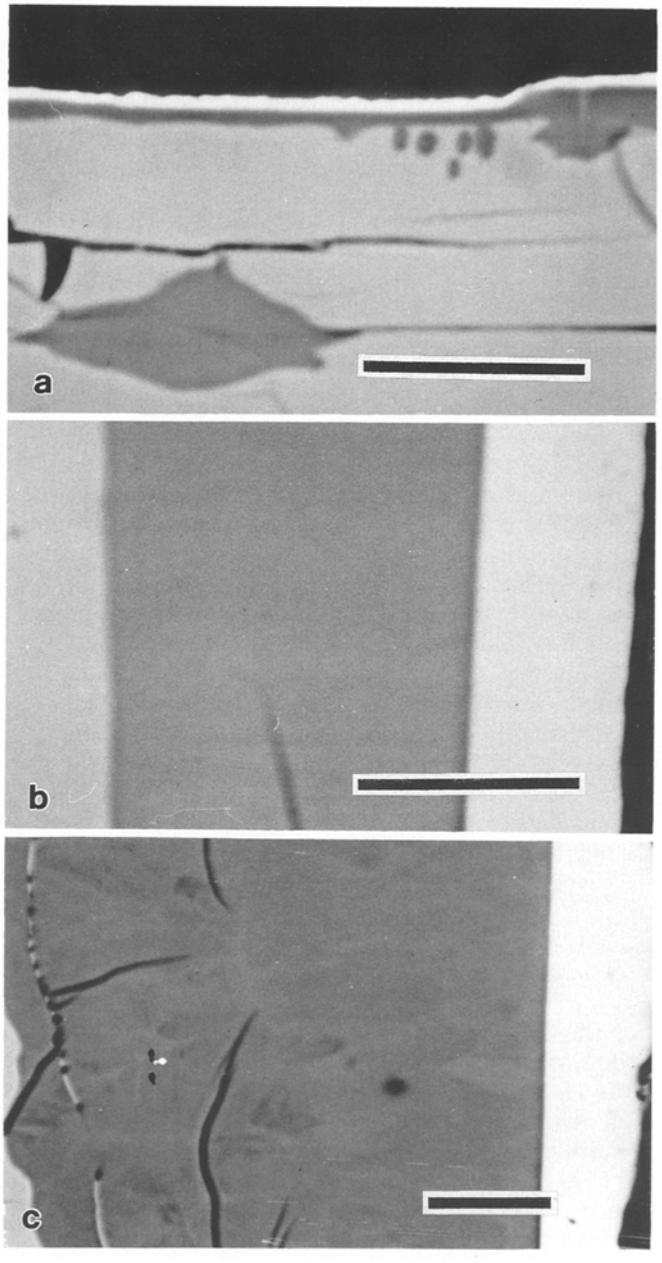

Fig. 3. BEI micrographs of cross sections of samples that have been oxidized in air at 770° C, for **a** 1 h, **b** 10 h, **c** 100 h. The white region is the external hematite layer, the gray region is the unreacted fayalite and the dark intermediate region is the two-phase layer containing iron oxide plus silica. 10 μm scale bars are shown in the lower right of each micrograph; note the smaller scale bar in **c**

Experimental Results

1. Oxidized in air

After the fayalite samples had been oxidized in air at 770° C, observations indicated that the initially polished surfaces were covered with a porous granular layer of iron oxide (Fig. 2a–c). With increase in the oxidation time, the grains of oxide became coarser. Based on the oxygen fugacity conditions during oxidation and the shape of the grains, the surficial iron oxide was identified as hematite (Fe_2O_3). No silicon peak could be found in the energy dispersive x-ray spectrum (EDS) of the sample surface.

When the samples were cut in half and polished, clear compositional layers could be seen optically and using the backscattered electron imaging (BEI) mode of the scanning electron microscope (SEM) (Fig. 3a–c). In this mode, regions of high average atomic weight appear light and regions of low average atomic weight appear dark. The white external layer is single-phase iron oxide, the light gray region is unaltered fayalite, and the dark intermediate region is a two-phase layer containing iron oxide and silica. Even at high magnification in the scanning electron imaging (SEI) mode of the SEM, separate phases could not be resolved in the two-phase region, although this region did appear mottled. The average thicknesses of the two-phase region and the external oxide layer increased with the time of oxidation, although the rate of growth slowed with increasing time (Table 1, Fig. 4). A clear correlation exists between the thickness of the two-phase region and that of the external oxide layer, with the former being about a factor of

Table 1. Fayalite oxidation at 770° C in air

Time (h)	External oxide thickness (μm)	Two-phase layer thickness (μm)	Δx (μm)
1	0.6±0.5	1±0.5	2±1
3	2 ±1	7±1	9±2
10	7 ±2	20±5	27±7
30	8 ±4	26±8	34±12
100	15 ±6	50±20	65±26

Table 2. Fayalite oxidation at 1030° C in CO/CO_2

Time (h)	External oxide thickness (μm)	Two-phase layer thickness (μm)	Δx (μm)
0.1	1±0.5	0.2±0.5	1±1
1	3±1	11 ±1	14±2
4.2	15±6	64 ±5	79±11
10	25±6	130 ±8	155±14
69.2		Sample fully oxidized	

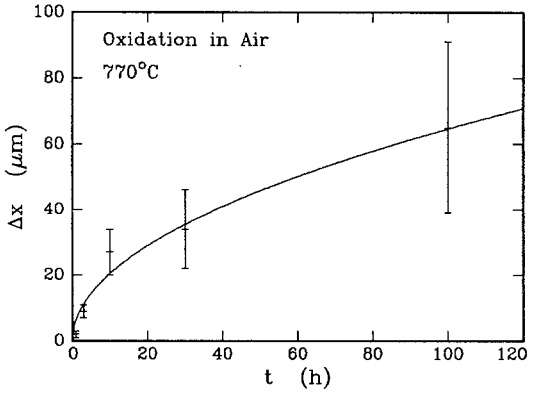

Fig. 4. Plot of Δx, the total thickness of the oxidation products of the fayalite, as a function of time for the specimens that were oxidized in air at 770° C. The fit to the data, shown by the solid line, yields a parabolic rate constant of $k_p \sim (6 \pm 2) \times 10^{-15}$ m^2 s^{-1}

3.5 larger than the latter. The thicknesses of both zones are quite variable within individual samples, especially in the shortest experiments, as reflected by the error bars in the data. Because the external oxide layer is quite friable, material may have been lost during polishing, adding a degree of uncertainty to the measurement. The porosity of this layer decreased in the longer experiments, particularly near the boundary with the two-phase region. Although some cracks were observed to penetrate through the oxidized regions into the fayalite, the general lack of oxidation along them (Fig. 3a–c) suggests that they formed during quenching from temperature. One rare exception to this observation is the two-phase zone in the lower left of Fig. 3a.

2. *Oxidized in CO/CO_2*

As in the oxidation experiments performed in air, the surfaces of the samples that had been oxidized in CO/CO_2 were coated in a porous layer of iron oxide; the grains in this layer coarsened with time at temperature (Fig. 5a–c). The shape of the oxide grains clearly identifies them as having the spinel (cubic) crystal form of magnetite (Fe_3O_4). There are notable morphology contrasts in the surface of the magnetite layer, with regions containing well-

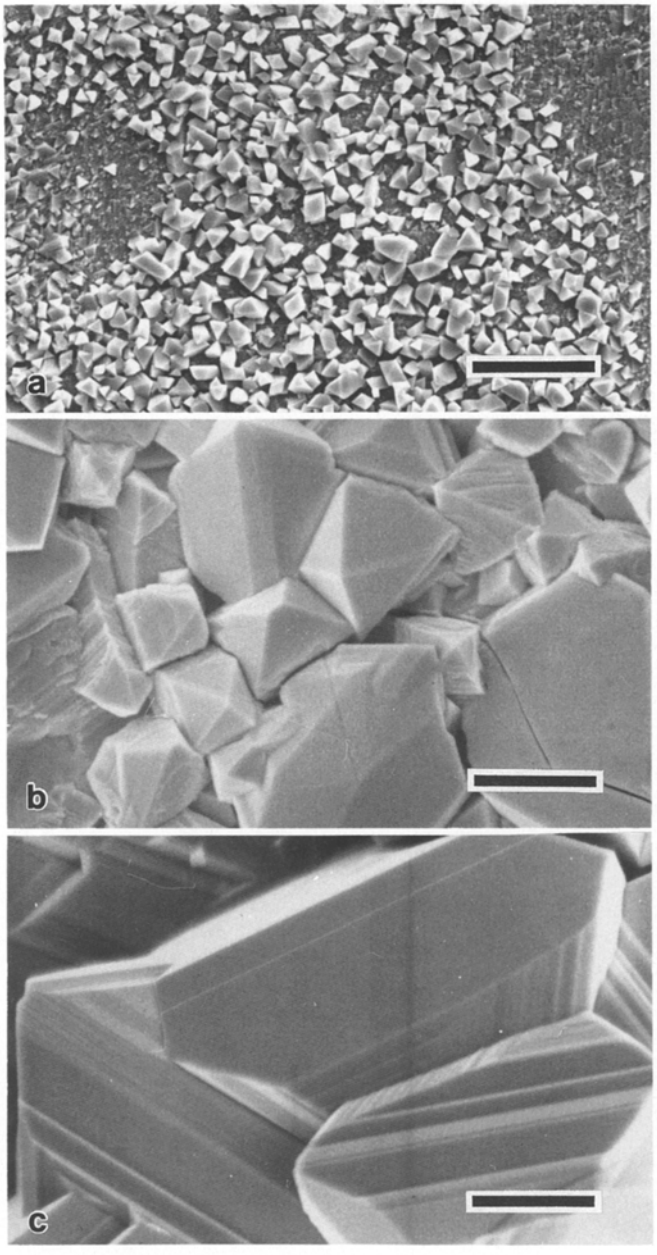

Fig. 5. SEI micrographs of the surfaces of samples that have been oxidized in a CO/CO_2 gas mixture at 1030° C, providing an oxygen fugacity within the magnetite stability field, for **a** 0.1 h, **b** 4.2 h, **c** 69.2 h. 10 μm scale bars are shown in the lower right of each micrograph

formed crystals and flat regions with little surface relief (Fig. 5a). No silicon peak could be found in the EDS on the SEM, indicating that there is no silica in the surface layer.

In cross-section, the compositional layers observed in BEI were similar to those in the air-oxidized specimens (Fig. 6a–c). However, there were two distinct phases visible within the two-phase layer; the black phase, shown most clearly in Fig. 6c, has been identified using the electron microprobe as silica and the light phase as magnetite. Both phases coarsen in grain size with increasing duration of the experiment. The grey region is pristine fayalite. The boundary between the two-phase region and the fayalite is sharp and linear, particularly in the longer time experiments. A thin discontinuous layer of silica, which could be seen between the two-phase region and the magnetite, increases in thickness with increasing

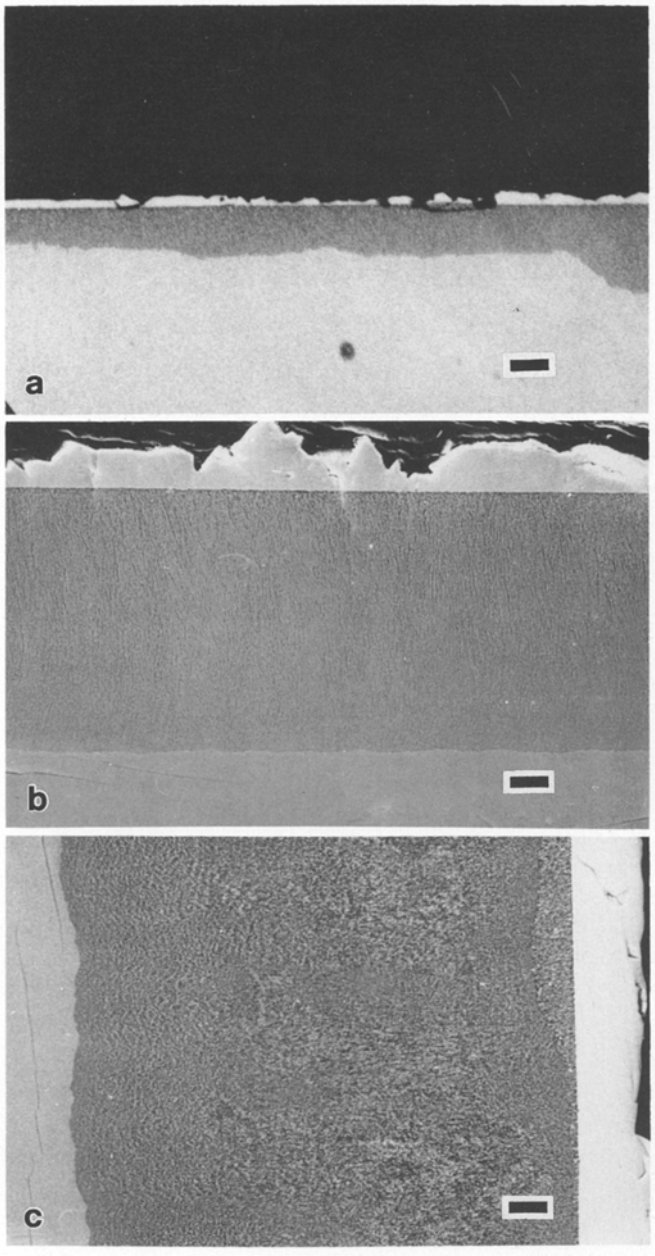

Fig. 6. BEI micrographs of cross sections of samples that have been oxidized in a CO/CO_2 gas mixture at 1030° C, providing an oxygen fugacity within the magnetite stability field, for **a** 1 h, **b** 4.2 h, **c** 10 h. The white region is the external magnetite layer, the gray region is the unreacted fayalite and the dark intermediate region is the two-phase layer containing iron oxide plus silica. 10 μm scale bars are shown in the lower right of each micrograph

time. The two-phase region and the extenal magnetite layer also increase in thickness with increasing time. Average values and error bars for the thickness of each layer in all of the CO/CO_2 experiments are given in Table 2 and plotted in Fig. 7.

Discussion

1. Oxidized in air

Electron microscopy observations of the specimens that had been oxidized in air at 770° C show clear compositional layering for all of the experimental durations. The

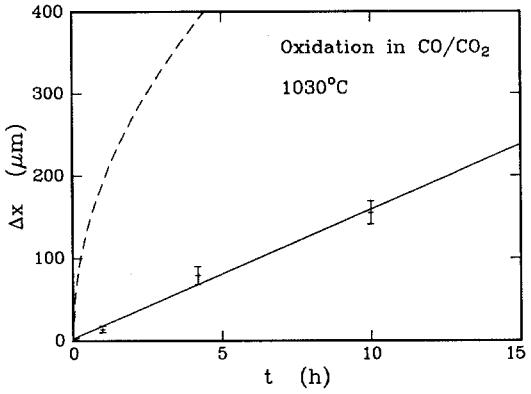

Fig. 7. Plot of Δx, the total thickness of the oxidation products of the fayalite, as a function of time for the specimens that were oxidized in a CO/CO_2 gas mixture at 1030° C, providing an oxygen fugacity within the magnetite stability field. The data fit a straight line, shown as the solid line, indicating interface rather than diffusion control of the oxidation. The dashed curve corresponds to the growth of a magnetite layer on wüstite at 1030° C, where the kinetics are rate limited by the diffusion of iron within the magnetite (5×10^{-12} m^2 s^{-1}) (Backhaus-Ricoult and Dieckmann 1986)

presence of a single-phase oxide layer external to the original surface, as indicated by the absence of silica, requires that the oxidation proceeds by the transport of iron to the gas-solid interface and that the oxygen atoms form an essentially immobile sublattice. The grain size of the interior iron oxide plus silica two-phase region is too small to be resolved in the scanning electron microscope. Grain coarsening was much more limited in the air-oxidized samples than in the other suite of experiments, because of the much lower oxidation temperatures in the former case (770° versus 1030° C).

Figure 3 shows only three clear compositional layers, an external oxide layer, an internal iron oxide plus silica layer, and the unreacted fayalite. Given the low contrast in atomic weight density between a $Fe_2O_3+SiO_2$ layer (3,700 kg/m^3) and a $Fe_3O_4+SiO_2$ layer (3,500 kg/m^3), and between a Fe_2O_3 layer (5,270 kg/m^3) and a Fe_3O_4 layer (5,200 kg/m^3), compared to the contrast between the two-phase region, the external oxide layer and the unreacted fayalite (4,390 kg/m^3), it is possible that the two-phase region contains zones of $Fe_2O_3+SiO_2$ and $Fe_3O_4+SiO_2$, or that the external oxide contains zones of Fe_2O_3 and Fe_3O_4 that were not discriminated in the scanning electron microscope. It is also possible that, due to the kinetics of oxidation, one of the layers is too thin to be resolved.

Although the number of data points is limited, the rate of oxidation clearly decreases with increasing time (Fig. 4). A fit of the data for the total thickness of the two-phase layer plus the external oxide layer as a function of time at 770° C to a parabolic growth law (Eq. (3)) yields a value for the parabolic rate constant of $k_p=(6\pm2)\times10^{-15}$ m^2 s^{-1}, as indicated by the solid line in Fig. 4. As discussed in the kinetics section, a parabolic law indicates that the oxidation process is predominantly diffusion rather than interface controlled.

Comparison may be made between the textures from the oxidation of fayalite and those measured from the

oxidation of iron and wüstite in air at similar temperatures. The experiments on the oxidation of iron and wüstite in air (Païdassi 1958a, b; Païdassi and Lopez 1958) and predictions based on oxidation kinetics (Atkinson and Taylor 1985) using the model of Yurek et al. (1974) show that the magnetite layer is about a factor of 5 times thicker than the hematite layer. In addition, the growth of hematite and magnetite layers on wüstite oxidized in air gives a parabolic rate constant of $k_p \sim 6 \times 10^{-13}$ m^2 s^{-1} at 770° C (Païdassi 1958a), which is a factor of 100 faster than observed in the oxidation of fayalite. However, the presence of SiO_2 as a product phase in the oxidation of fayalite and the different oxygen stability limits for fayalite compared to iron or wüstite, must affect the kinetics of oxide growth and the relative thicknesses of the various layers.

The chemical potential gradient across the layer(s) containing magnetite in the oxidized fayalite will be significantly less than in oxidized wüstite due to the higher oxygen activity at the quartz-fayalite-magnetite phase boundary (4×10^{-16} atm at 770° C) than at the wüstite-magnetite phase boundary (3×10^{-19} atm at 770° C) (Fig. 1) and due to the increased width of the two-phase zone resulting from the presence of SiO_2. In addition, if a layer containing $Fe_2O_3 + SiO_2$ exists in the oxidized fayalite, the chemical potential gradient of oxygen across this zone will be smaller than that across the hematite layer formed during the oxidation of wüstite in air due to the presence of the SiO_2 phase. Assuming that the diffusive transport of iron through an iron oxide plus silica layer is essentially the same as that through a pure iron oxide layer, the ratio of thicknesses of the hematite-bearing layers to the magnetite-bearing layers resulting from the oxidation of fayalite should be smaller than in the case of wüstite oxidation (1:5). Thus, it is possible that the boundary between the hematite-bearing layer(s) and the magnetite-bearing layers occurs approximately at the original surface so that a single-phase Fe_2O_3 layer overlies a two-phase $Fe_3O_4 + SiO_2$ layer. This possibility is in accord with the BEI observations that show only two compositional layers (although, as discussed above, a third layer may not have been discernible in the SEM). Also, the ratio of the external oxide thickness to that of the two-phase region is about 1:3.5, in reasonable accord with the predictions from the comparison with the oxidation of wüstite.

It is also worthy of note that, as in the case of the oxidation of iron and wüstite (Atkinson and Taylor 1985), the kinetics of growth of the oxide layers is significantly faster than would be expected on the basis of the measured diffusion rates in magnetite (Dieckmann and Schmalzried 1977) and hematite (Hoshino and Peterson 1985a, b; Atkinson and Taylor 1985). Consequently, it seems likely that the growth rate is defined not by the diffusion of iron defects through the lattice of the iron oxides but by the diffusion of iron defects along fast diffusion paths, such as grain boundaries in the oxidized layers. The slower rate of growth than for the oxidation of wüstite under similar conditions probably reflects the lower driving force for diffusion (the oxygen chemical potential gradient) and, possibly, slower diffusion rates along boundaries between iron oxide and silica.

2. *Oxidized in CO/CO_2*

As in the experiments conducted in air, the presence of a single-phase iron oxide (magnetite) layer external to the original surface of the fayalite indicates that, in CO/CO_2 at 1030° C, the oxidation of fayalite proceeds by the transport of iron to the gas-solid interface and that the oxygen atoms from an immobile sublattice. Despite the limited number of data points, it is evident from Fig. 7 that the total thickness of the two-phase layer plus the external oxide layer increases linearly rather than parabolically with time, giving a linear rate constant of $k_l \sim (4.4 \pm 0.3) \times 10^{-9}$ m s^{-1} using Eq. (4). At a temperature of 1030° C, the total thickness of the reacted zone Δx, predicted from the calculations of Backhaus-Ricoult and Dieckmann (1986) for the oxidation of wüstite using the data of Dieckmann and Schmalzried (1977) for iron diffusion in magnetite, would be approximately 1050 μm after 10 h, compared to the measured value of 155 μm for the oxidation of fayalite. Thus, the kinetics of the oxidation of fayalite is not only linear with time but is also much slower than would be expected if the oxidation was rate-limited by the diffusion of iron from the internal fayalite-two-phase interface through the magnetite plus silica and magnetite layers to the surface.

A deviation from parabolic oxidation kinetics was also observed by Dieckmann et al. (1981), Backhaus-Ricoult and Dieckmann (1986) and Dieckmann (1987) for the oxidation of wüstite to magnetite. In these earlier studies, the kinetics of the oxidation of wüstite was also considerably slower than predicted on the basis of the data on diffusion of iron in magnetite (Backhaus-Ricoult and Dieckmann 1986; Dieckmann and Schmalzried 1977). These slower kinetics and the deviation from parabolic behavior were attributed to interface control of the oxidation process at the gas-solid interface. It is unlikely that the oxidation of fayalite is rate-controlled by diffusion through the thin silica layer that grows between the external oxide and the two-phase region, as this layer coarsens and thickens with time and would also be expected to give a parabolic dependence of layer thickness on time. Thus, parallel to the wüstite oxidation experiments of Dieckmann et al. (1981), Backhaus-Ricoult and Dieckmann (1986) and Dieckmann (1987), the oxidation is most likely rate limited by the reaction at the gas-solid interface.

Conclusions

1. The oxidation of fayalite proceeds by the diffusion of iron from the internal interface between the unoxidized fayalite and the oxidation products to the external oxide-gas interface. Silicon and oxygen are essentially immobile at temperatures to 1030° C.

2. An external single-phase iron oxide layer overlying an internal iron oxide plus silica layer forms during the oxidation of fayalite in air at 770° C. The kinetics of the oxidation process follow a parabolic form, suggesting that the diffusion of iron through the oxidized layers rate limits the oxide growth. This diffusive transport of iron probably has some component due to fast transport paths, such as along grain boundaries.

3. During the oxidation of fayalite within the magnetite stability field using a CO/CO_2 gas mixture at 1030° C, an external single-phase magnetite layer forms over a two-phase magnetite plus silica layer. The grains of magnetite and silica in the oxidized region coarsen with increasing duration of the experiments. The rate of growth of the oxide follows a linear rate law and is relatively slow compared to the rate predicted for diffusion-controlled growth, suggesting that oxidation is rate limited by the reaction at the gas-solid interface.

Acknowledgements. Support of the National Science Foundation through grants EAR-8318933 and EAR-9018044 is gratefully acknowledged. The scanning electron microscopy was performed in the electron microscope facility of the Materials Science Center at Cornell, staffed by John Hunt, Ray Coles, and Margaret Craft. I am grateful to Ron Black who assisted with much of the experimental work and to David Kohlstedt for his support and for many fruitful discussions. The manuscript benefitted from a careful review by Rudi Dieckmann, and discussions with Darby Dyar and Diana Fisler.

References

Atkinson A, Taylor RI (1985) Diffusion in ^{55}Fe in Fe_2O_3 single crystals. J Phys Chem Solid 46:469–475

Backhaus-Ricoult M, Dieckmann R (1986) Defects and cation diffusion in magnetite (VII): diffusion-controlled formation of magnetite during reactions in the iron-oxygen system. Ber Bunsenges Phys Chem 90:690–698

Dieckmann R, Schmalzried H (1977) Defects and cation diffusion in magnetite (II). Ber Bunsenges Phys Chem 81:414–419

Dieckmann R, Schmalzried H, Mason TO (1981) Kinetics of dense magnetite formation during oxidation of wüstite and reduction of hematite in CO/CO_2 gas mixtures. Arch Eisenhuttenwes 52:211–218

Dieckmann R (1982) Defects and cation diffusion in magnetite (IV): nonstoichiometry and point defect structure of magnetite. Ber Bunsenges Phys Chem 86:112–118

Dieckmann R (1987) Diffusion of cations and of point defects in magnetite ($Fe_{3-\delta}O_4$). In: Dayananda MA, Rothman SJ, King WE (eds) Oxidation of metals and associated mass transport. The Metallurgical Society, Warrendale, Pennsylvania, pp 7–28

Finch CB, Clark GW, Kopp OC (1980) Czochralski growth of single-crystal fayalite under controlled oxygen fugacity conditions. Am Mineral 65:381–389

Gaite JM, Hafner SS (1984) Environment of Fe^{3+} at the M2 and Si sites of forsterite obtained with EPR. J Chem Phys 80:2747–2751

Garnaud G, Rapp RA (1977) Thickness of oxide layers formed during the oxidation of iron. Oxid Metals 11:193–198

Hoshino K, Peterson NL (1985a) Cation self-diffusion and the isotope effect in $Fe_2O_3{}^+$. J Phys Chem Solid 46:375–382

Hoshino K, Peterson NL (1985b) Cation self-diffusion and impurity diffusion in $Fe_2O_3{}^+$. J Phys Chem Solid 46:1247–1254

Houlier B, Cheraghmakani M, Jaoul O (1990) Silicon diffusion in San Carlos olivine. Phys Earth Planet Inter 62:329–340

Jaoul O, Poumellec M, Froidevaux C, Havette A (1981) Silicon diffusion in forsterite: a new constraint for understanding mantle deformation. In: Stacey FD, Paterson MS, Nicolas A (eds) Anelasticity in the Earth: Geodynamics Series, Vol 4. American Geophysical Union, Washington, pp 95–100

Kubaschewski O, Hopkins BE (1953) Oxidation of Metals and Alloys. Butterworths, London

Nakamura A, Schmalzried H (1983) On the nonstoichiometry and point defects of olivine. Phys Chem Minerals 10:27–37

O'Neill HStC (1987) Quartz-fayalite-iron and quartz-fayalite-magnetite equilibria and the free energy of formation of fayalite (Fe_2SiO_4) and magnetite (Fe_3O_4). Am Mineral 72:67–75

O'Neill HStC (1988) Systems Fe–O and Cu–O: thermodynamic data for the equilibria Fe–"FeO," Fe–Fe_3O_4, "FeO"–Fe_3O_4, Cu–Cu_2O, and Cu_2O–CuO from emf measurements. Am Mineral 73:470–486

Païdassi J (1958a) Sur la cinetique de l'oxydation du fer dans l'air dans l'intervalle 700–1250° C. Acta Metall 6:184–194

Païdassi J (1958b) Sur l'oxydation du protoxyde de fer dans l'air dans l'intervalle 600–1350° C. Acta Metall 6:219–221

Païdassi J, Lopez J (1958) Sur quelques particularites de l'oxydation de la magnetite dans l'air dans l'intervalle 400–1350° C. Acta Metall 6:221–223

Ricoult DL, Kohlstedt DL (1985) Creep of Fe_2SiO_4 and Co_2SiO_4 single crystals in controlled thermodynamic environments. Philos Mag A51:79–93

Sato H (1986) High temperature A.C. electrical properties of olivine single crystal with varying oxygen partial pressure: implications for the point defect chemistry. Phys Earth Planet Inter 41:269–282

Schmalzried H (1983) Internal and external oxidation of nonmetallic compounds and solid solutions (I). Ber Bunsenges Phys Chem 87:551–558

Schock RN, Duba AG (1984) Point defects and the mechanisms of electrical conduction in olivine. In: Schock RN (ed) Point Defects in Minerals, Geophys Monogr Ser, Vol 31, Am Geophys Union, Washington, DC, pp 88–96

Wu T, Kohlstedt DL (1988) Rutherford backscattering spectroscopy study of the kinetics of oxidation of $(Mg,Fe)_2SiO_4$. J Am Ceram Soc 71:540–545

Yurek GJ, Hirth JP, Rapp RA (1974) The formation of two-phase layered scales on pure metals. Oxid Metals 8:265–281